WWW.IJRPR.COM

International Journal of Research Publication and Reviews

Journal homepage: www.ijrpr.com ISSN 2582-7421

RFID-Based EV Charging Station Using Renewable Energy

[Banrjee Shomit Sanjay][1], [Kishor Eknath Doke][2]and [Dhanshri Shantaram Dhanwate][3]

Department of Electrical Engineering, NIT's Late Annasaheb Patil Polytechnic,Nashik,Maharashtra,India
banarjeeshomit2@gmail.com, kishordoke162@gmail.com, *dhanshridhanwate96@gmail.com*

ABSTRACT—

The rapid adoption of electric vehicles (EVs) demands charging infrastructure that is secure, automated and environmentally sustainable. This paper presents the design and simulation of an RFID-based EV charging station powered by solar photovoltaic (PV) energy. A 3 kWp PV array feeds a 51.2 V, 6.14 kWh $LiFePO_4$ battery bank through an MPPT charge controller, and a two-bay constant-current/constant-voltage (CC–CV) charger supplies light electric vehicles. User authentication, prepaid billing and session control are implemented with an MFRC522 RFID reader interfaced to an ESP32 microcontroller, while current, voltage and temperature sensing provide protection and energy metering. The system is sized from the daily energy demand and local insolation and is evaluated with an hour-by-hour energy-balance simulation over one year. The results show that the station meets 82% of its annual demand from solar energy, imports only 687 kWh from the grid and avoids about 2.2 t of CO_2 per year compared with a grid-only station. The design is low-cost, modular and suitable for semi-urban deployment.

Index Terms—Electric vehicle, RFID, solar photovoltaic, MPPT, battery storage, charging station, ESP32.

I. INTRODUCTION

Transport electrification is a key strategy for reducing urban air pollution and dependence on imported fuel. Mo re than 14 million electric cars were registered worldwide in 2023, and the growth is led by two- and three-wheelers in many Asian markets [1]. In India, the Ministry of Power has issued guidelines and standards that encourage widespread public charging infrastructure [2]. For small cities and semi-urban areas, however, installing grid-connected charging points is hampered by limited feeder capacity, unreliable supply and the risk of unauthorized or unmetered use.

Conventional charging points are usually operated manually, with a fixed tariff and a human attendant for payment. This increases operating cost and makes it difficult to track energy use per customer. Radio-frequency identification (RFID) provides a simple, inexpensive and contactless way to identify each user, to enable prepaid billing and to record every charging session. At the same time, powering the station from solar PV reduces the carbon footprint of the charged energy and lowers the electricity bill.

This paper proposes an RFID-based EV charging station that is supplied mainly by a solar PV–battery system. The main contributions are: (i) a complete architecture combining PV generation, battery storage, a CC–CV charger and an RFID access-control unit; (ii) design equations used to size the PV array and battery from the daily charging demand; (iii) a control algorithm for authentication, metering, billing and protection; and (iv) a year-long hourly energy-balance simulation that quantifies solar share, grid dependence and CO_2 savings.

The rest of the paper is organized as follows. Section II reviews related work, Section III describes the system architecture, Section IV presents the design methodology, Section V explains the working algorithm, Section VI discusses the results and Section VII concludes the paper.

II. RELATED WORK

Reviews of charger topologies and power levels show that low-power on-board and off-board chargers are the most practical option for light electric vehicles, while fast chargers place heavy demands on the distribution network [3]. Studies on rapid-charge stations point out that their peak load can stress the local grid, which motivates local generation and storage [4]. RFID technology, standardized for 13.56 MHz proximity cards under ISO/IEC 14443, is widely used for access control and e-payment because of its low cost, fast reading time and the ability to store a unique identifier on every card [5]. Low-cost reader integrated circuits such as the MFRC522 make this technology easy to interface with microcontrollers [6]. Many reported RFID charging prototypes, however, rely only on the utility supply. The present work combines RFID-based user management with a renewable source and battery buffer, and evaluates the energy balance quantitatively.

III. SYSTEM ARCHITECTURE

A. Overall Architecture

The proposed station is shown in Fig. 1. The top row is the power path: the PV array supplies an MPPT charge controller, which charges the battery bank and feeds a common 51.2 V DC bus. Two independent CC–CV charger modules convert the bus voltage into the 67.2 V, 10 A output required by

a 60 V (16-cell) lithium-ion e-scooter pack. A grid-connected AC–DC supply acts as a backup and takes over automatically when the battery state of charge (SoC) falls to its lower limit. The bottom row is the control path: an RFID reader identifies the user, an ESP32 microcontroller takes the decision, and relays connect the selected bay to the charger only for authenticated users.

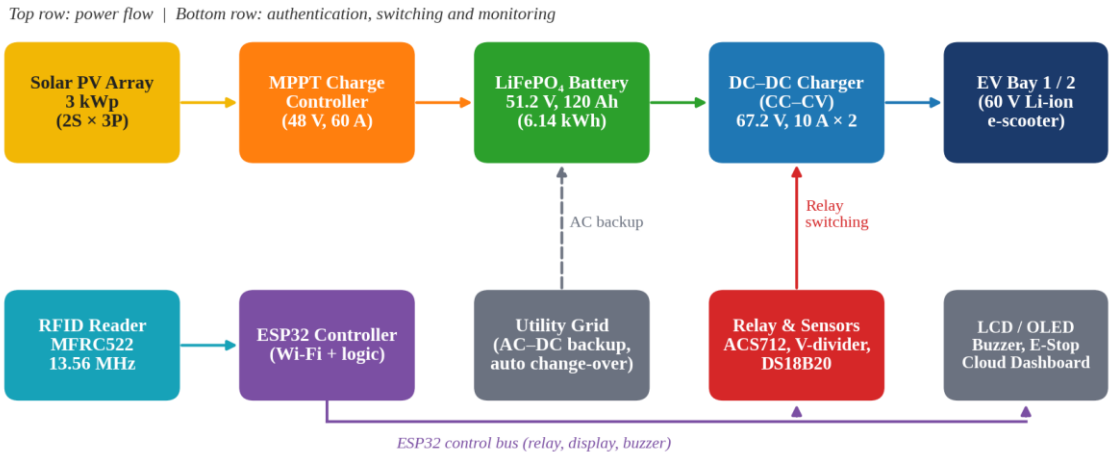


Fig. 1. Block diagram of the proposed RFID-based EV charging station using solar PV, battery storage and grid backup.

B. Solar PV Array and MPPT Controller

The array consists of six 500 Wp mono-crystalline modules arranged as two series strings in three parallel branches (2S × 3P). With a typical module open-circuit voltage of about 49 V and short-circuit current of about 13.9 A, the array gives roughly 98 V and 42 A, which is inside the 150 V / 60 A rating of the MPPT controller. The single-diode model of a PV module [8] relates the output current to the irradiance and cell temperature, and the maximum power point moves with both. A maximum power point tracking (MPPT) algorithm such as perturb-and-observe or incremental conductance keeps the array at its optimum operating point and increases the harvested energy compared with direct connection [9].

C. Battery Energy Storage

A 51.2 V, 120 Ah lithium iron phosphate ($LiFePO_4$) battery with an integrated battery management system (BMS) stores the surplus solar energy. $LiFePO_4$ was chosen for its long cycle life, flat discharge curve and good thermal stability compared with lead–acid batteries [10]. The usable depth of discharge (DoD) is limited to 80%, which keeps a 20% reserve and extends battery life.

D. RFID Authentication Module

The MFRC522 reader operates at 13.56 MHz and communicates with the ESP32 over the SPI bus. Each registered user holds a MIFARE Classic 1K card or tag whose 4-byte unique identifier (UID) is stored in the controller memory together with the prepaid balance in rupees. When a card is brought near the reader, the controller compares its UID with the registered list; unregistered cards are rejected and a buzzer sounds. The reading time is a fraction of a second, so authentication does not delay charging [5], [6].

E. Controller, Sensing and Protection

An ESP32 DevKit (dual-core, Wi-Fi enabled) is the central controller [7]. Charging current is measured with an ACS712-30A Hall-effect sensor, output voltage with a resistive divider and pack temperature with a DS18B20 digital sensor. A 128 × 64 OLED shows the user name, balance, energy and cost, and a push-button emergency stop opens the relays at once. The protection thresholds are over-voltage at 68 V, over-current at 12 A and over-temperature at 55 °C. Table I lists the main design specifications and Table II gives the pin connections.

TABLE I

Design Specifications of the Station

Parameter	Specification
PV array	3 kWp (6 × 500 Wp), 2S × 3P
MPPT controller	48 V class, 60 A, $V_{oc,max}$ 150 V
Battery bank	51.2 V, 120 Ah $LiFePO_4$; 6.14 kWh; DoD 80%
Charger outputs	2 bays, CC–CV, 67.2 V / 10 A each
Controller	ESP32 DevKit, Wi-Fi, 12-bit ADC
RFID	MFRC522, 13.56 MHz, ISO/IEC 14443A
Sensing	ACS712-30A, voltage divider, DS18B20
Design demand	8 sessions/day × 1.2 kWh = 9.6 kWh/day

TABLE II

ESP32 Pin Connections

Module	Signal	ESP32 pin
MFRC522	SDA / SCK	GPIO5 / GPIO18
MFRC522	MOSI / MISO	GPIO23 / GPIO19
MFRC522	RST	GPIO17
Relay 1 / 2	IN1 / IN2	GPIO26 / GPIO27
ACS712 (via divider)	OUT	GPIO34 (ADC)
Voltage divider	V_{out}	GPIO35 (ADC)
DS18B20	DATA	GPIO4
OLED (I²C)	SDA / SCL	GPIO21 / GPIO22
Buzzer / E-stop	OUT / IN	GPIO25 / GPIO13

IV. DESIGN METHODOLOGY

A. Energy Demand and PV Sizing

The station is designed for N = 8 charging sessions per day with an average delivered energy of E_s = 1.2 kWh per session (a 60 V, 20 Ah pack). Including the charger efficiency $\eta_c = 0.92$ and the battery round-trip efficiency $\eta_b = 0.95$, the daily energy that the source must supply is

$$E_{req} = (N \cdot E_s) / (\eta_c \cdot \eta_b) = 10.98 \text{ kWh} \quad (1)$$

For an average of PSH = 5.5 peak sun hours per day [11], [12] and a performance ratio PR = 0.75 that accounts for temperature, wiring and dust losses, the required PV capacity is

$$P_{pv} = E_{req} / (PSH \cdot PR) = 2.66 \text{ kWp} \quad (2)$$

and a standard 3 kWp array (6 × 500 Wp) is selected, which gives a mean daily generation of 3 × 5.5 × 0.75 = 12.4 kWh.

B. Battery Sizing

About 40% of the daily demand is assumed to occur after sunset or in low-sun hours, so that the battery must supply $E_n = 0.4 \cdot E_{req}$. With DoD = 0.8, the nominal capacity is

$$C_b = E_n / (DoD \cdot \eta_b) = 5.78 \text{ kWh} \quad (3)$$

and the nearest practical size, 51.2 V × 120 Ah = 6.14 kWh, is chosen.

C. Metering and Billing

During a session the controller samples voltage V and current I every 100 ms. The delivered energy and the bill are calculated as

$$E_{sess} = \int V(t) \cdot I(t)\, dt, \quad Cost = E_{sess} \times T_{kWh} \quad (4)$$

where T_{kWh} is the configurable tariff in rupees per kWh. The pack SoC during CC charging is estimated by coulomb counting as

$$SoC(t) = SoC_0 + (1/C_n) \int I\, dt \quad (5)$$

where C_n is the rated capacity of the vehicle battery. In the CC–CV method the charger holds a constant current of 0.5 C (10 A) until the pack voltage reaches 67.2 V, then holds the voltage and lets the current taper down to the 1 A cut-off, after which the session ends.

D. Energy Dispatch Rules

For every hour the PV power first supplies the charging load directly. Any surplus is stored in the battery until it is full (100% SoC); further surplus is curtailed. When the PV power is less than the load, the battery supplies the deficit until the SoC reaches the 20% limit, after which the grid backup supplies the remaining demand. These rules are used in the simulation of Section VI.

V. SOFTWARE DESIGN AND WORKING

The firmware, written in the Arduino framework for the ESP32, follows the flowchart of Fig. 2. After initialization the system waits for a card. A valid UID with a balance above the minimum (set to ₹20) closes the relay of a free bay and starts the CC–CV charger. During charging the controller updates the energy and cost every second, shows them on the OLED and checks the protection limits. The session is ended when the battery is full (current below 1 A), when the prepaid balance is exhausted, when a fault occurs or when the user scans the card again. The relay is then opened, the final bill is deducted from the card balance and the session record (UID, start time, energy, cost) is stored. If Wi-Fi is available, the record is also published to a cloud dashboard through MQTT for remote monitoring.

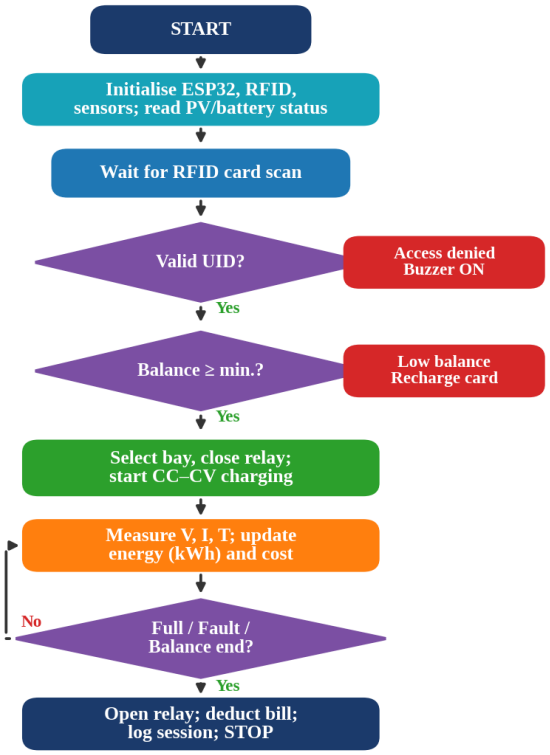


Fig. 2. Flowchart of RFID authentication, charging control and billing.

VI. RESULTS AND DISCUSSION

A. Simulation Setup

The performance was evaluated with a Python hour-by-hour energy-balance model of the design in Table I over 365 days. Monthly insolation values of 4.3–7.0 peak sun hours were taken as representative of western-central India at about 18°N [12]. To represent the monsoon, 45–60% of the days in June–September were modelled as overcast with only 30% of normal PV output, and 6–20% in other months. The demand profile has a morning peak (08:00–10:00) and a stronger evening peak (17:00–19:00). The battery SoC limits are 20–100%, the grid emission factor is assumed to be 0.71 kg CO_2/kWh in line with the CEA baseline database [13], and PR = 0.75. The values are model results and not field measurements.

B. Daily Operation

Fig. 3 shows a typical day. The PV power starts at about 06:30, peaks near 1.8 kW at noon and totals 12.4 kWh. Between 09:00 and 15:00 the PV output exceeds the charging demand, so the battery charges from about 30% to 100% SoC. In the evening peak the battery supplies the load and the SoC falls to its daily minimum of 28%, well above the 20% reserve. On such an average day no grid energy is required.

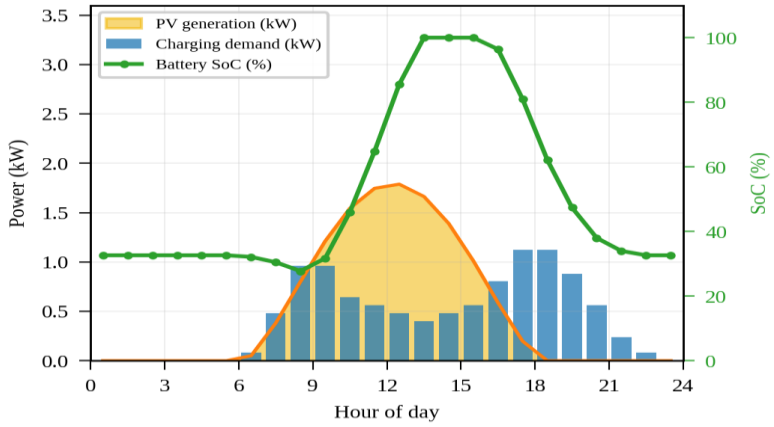


Fig. 3. Hourly PV generation, charging demand and battery SoC on an average day.

C. CC–CV Charging Behaviour

Fig. 4 shows the modelled charging curve of a 60 V, 20 Ah pack charged from 10% SoC. In the CC mode the current is 10 A and the voltage rises from 59.5 V to 67.2 V in 1.4 h, taking the pack to about 80% SoC. In the CV mode the current decays exponentially to the 1 A cut-off in 0.95 h. The complete charge takes about 2.35 h and delivers 1.14 kWh, which agrees with the design value of 1.2 kWh per session used in (1).

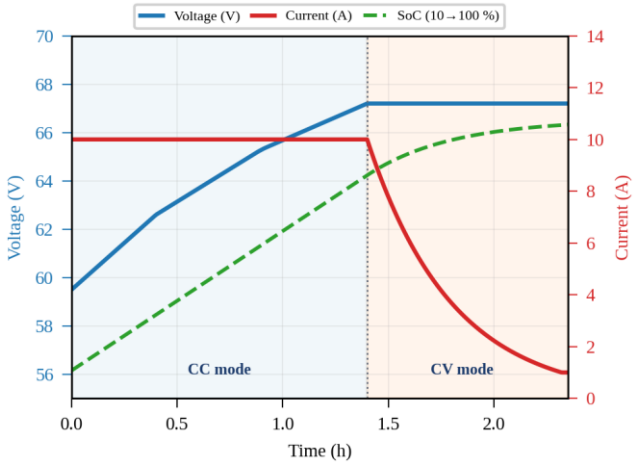


Fig. 4. Modelled CC–CV charging profile of a 60 V, 20 Ah Li-ion pack (voltage, current and SoC).

D. Annual Energy Performance

The monthly energy flows are plotted in Fig. 5 and summarized in Table III. The array generates 4401 kWh per year against a source-side demand of 3809 kWh. Of this demand, 2041 kWh (54%) is supplied directly by the PV array, 1081 kWh (28%) through the battery and 687 kWh (18%) by the grid, so the annual solar fraction is 82%. From October to May the solar fraction is 83–100%, and in March it reaches 100%. In the monsoon months (July–September) it drops to 60–63% because of long overcast spells, and the grid backup supplies the gap. The extra PV energy in the dry months (1224 kWh, 28% of generation) is curtailed because the battery is already full.

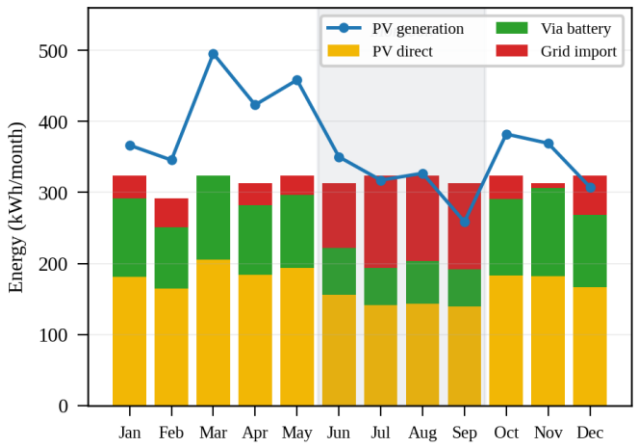


Fig. 5. Monthly PV generation and the share of demand supplied by PV, battery and grid.

TABLE III

Annual Simulation Results

Quantity	Value
PV generation	4401 kWh/yr
Source-side charging demand	3809 kWh/yr
Supplied directly by PV	2041 kWh (54%)
Supplied through battery	1081 kWh (28%)
Grid import	687 kWh (18%)
Curtailed PV energy	1224 kWh
Annual solar fraction	82%
Best / worst month	Mar (100%) / Jul (60%)
CO_2 avoided	2216 kg/yr

E. Environmental Impact and Comparison

Fig. 6 compares the annual emissions. A grid-only station delivering the same energy would emit about 2704 kg of CO_2, whereas the proposed station emits 488 kg, an avoided 2216 kg (82%) per year. Table IV compares the proposed design qualitatively with a conventional manually operated grid station and an RFID station powered only by the grid.

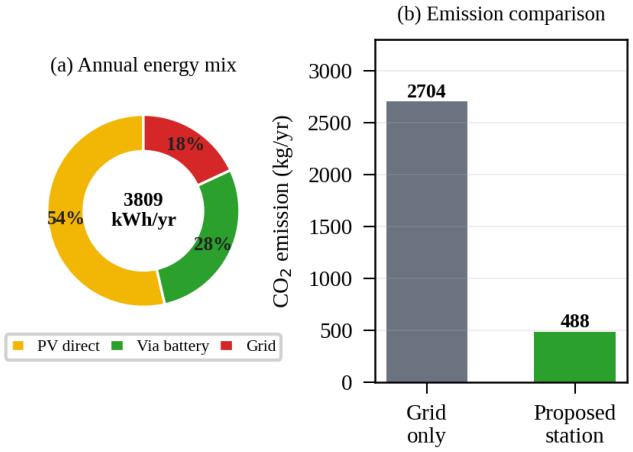


Fig. 6. (a) Annual energy mix and (b) CO_2 emissions of the proposed station compared with a grid-only station.

TABLE IV

Comparison of Charging Station Types

Feature	Conventional	RFID, grid-only	Proposed
User access	Manual	RFID card	RFID card
Billing	Attendant	Automatic	Automatic, prepaid
Energy source	Grid	Grid	Solar + battery + grid
Outage ride-through	No	No	Yes (battery)
Session log	None	Local	Local + cloud
CO_2 emission	Highest	Highest	82% lower

F. Sensitivity to PV and Battery Size

To check the design choice, the annual simulation was repeated for PV capacities of 2–5 kWp and battery capacities of 3.07–12.3 kWh, as shown in Fig. 7. With the selected 3 kWp array, a half-size battery (3.07 kWh) lowers the solar fraction to 70%, whereas doubling it to 12.3 kWh raises it only to 87%. Increasing the array from 3 to 5 kWp with the 6.14 kWh battery gives 88.5%. The curves flatten above about 6 kWh, so the selected combination is a good compromise between solar share and cost.

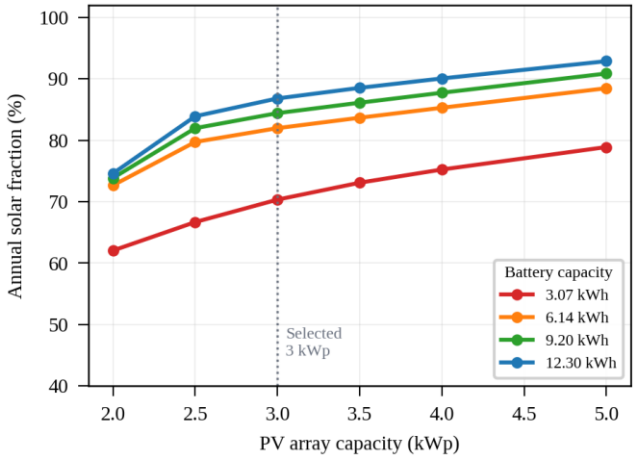


Fig. 7. Annual solar fraction versus PV capacity for four battery sizes.

G. Indicative Cost Estimate

Table V gives an indicative budget for the prototype based on approximate Indian market prices, excluding taxes and installation labour. The battery and PV modules account for about three-quarters of the cost, while the complete RFID and control electronics cost only about ₹3,500 (1.2% of the total). The RFID-based management features are therefore economical to add to any charging station.

TABLE V

Indicative Cost Estimate (INR, Approximate)

Item	Cost (₹)
PV modules, 6 × 500 Wp	85,000
MPPT charge controller, 60 A	15,000
$LiFePO_4$ battery 6.14 kWh with BMS	1,30,000
Two CC–CV charger modules	24,000
ESP32, MFRC522, sensors, relays, OLED	3,500
Mounting, cables, protection, enclosure	35,000
Total	**2,92,500**

H. Discussion

The results show that a modest 3 kWp array and a 6 kWh battery can serve most of the energy needs of a small two-bay station for light vehicles. The RFID unit adds very little cost and power consumption, while giving user identification, automatic billing and a complete session record. The main limitations are the lower solar fraction in the monsoon and the surplus energy that is wasted in the dry season. The latter can be used by adding more charging bays, a small battery-swapping unit, or by exporting power to the grid. The values in Section VI come from a simulation, and the model should be validated with measured data from the hardware prototype.

VII. CONCLUSION AND FUTURE SCOPE

This paper presented the design and simulation of an RFID-based EV charging station powered by solar PV with battery storage. The 3 kWp PV array, 6.14 kWh $LiFePO_4$ battery and two-bay CC–CV charger were sized from the daily demand using simple design equations, and an ESP32 with an MFRC522 reader provides secure authentication, metering, prepaid billing and protection. The annual simulation indicates a solar fraction of 82%, a grid import of 687 kWh and an avoided emission of about 2.2 t of CO_2 per year. Future work includes experimental validation on the prototype, use of the surplus energy through vehicle-to-grid or grid export, encrypted card authentication (for example MIFARE DESFire), mobile-app payment through UPI, and SoC prediction based on weather forecasts.

ACKNOWLEDGMENT

The author thanks the project guide and the Department of Electrical Engineering for their guidance and laboratory support.

REFERENCES

[1] International Energy Agency, “Global EV Outlook 2024,” IEA, Paris, France, 2024.

[2] Ministry of Power, Government of India, “Revised guidelines and standards for charging infrastructure for electric vehicles,” New Delhi, India, 2024.

[3] M. Yilmaz and P. T. Krein, “Review of battery charger topologies, charging power levels, and infrastructure for plug-in electric and hybrid vehicles,” *IEEE Trans. Power Electron.*, vol. 28, no. 5, pp. 2151–2169, May 2013.

[4] M. Etezadi-Amoli, K. Choma, and J. Stefani, “Rapid-charge electric-vehicle stations,” *IEEE Trans. Power Del.*, vol. 25, no. 3, pp. 1883–1887, Jul. 2010.

[5] K. Finkenzeller, *RFID Handbook: Fundamentals and Applications in Contactless Smart Cards, Radio Frequency Identification and Near-Field Communication*, 3rd ed. Chichester, U.K.: Wiley, 2010.

[6] NXP Semiconductors, “MFRC522: Standard performance MIFARE and NTAG frontend,” Data Sheet.

[7] Espressif Systems, “ESP32 series datasheet,” Shanghai, China.

[8] M. G. Villalva, J. R. Gazoli, and E. R. Filho, “Comprehensive approach to modeling and simulation of photovoltaic arrays,” *IEEE Trans. Power Electron.*, vol. 24, no. 5, pp. 1198–1208, May 2009.

[9] T. Esram and P. L. Chapman, “Comparison of photovoltaic array maximum power point tracking techniques,” *IEEE Trans. Energy Convers.*, vol. 22, no. 2, pp. 439–449, Jun. 2007.

[10] D. Linden and T. B. Reddy, Eds., *Handbook of Batteries*, 3rd ed. New York, NY, USA: McGraw-Hill, 2002.

[11] J. A. Duffie and W. A. Beckman, *Solar Engineering of Thermal Processes*, 4th ed. Hoboken, NJ, USA: Wiley, 2013.

[12] World Bank Group and Solargis, “Global Solar Atlas 2.0,” [Online]. Available: https://globalsolaratlas.info

[13] Central Electricity Authority, Ministry of Power, India, “CO_2 baseline database for the Indian power sector,” New Delhi, India.